# Competitive endogenous RNA is an intrinsic component of EMT regulatory circuits and modulates EMT

Liu et al.

## Supplementary Figures

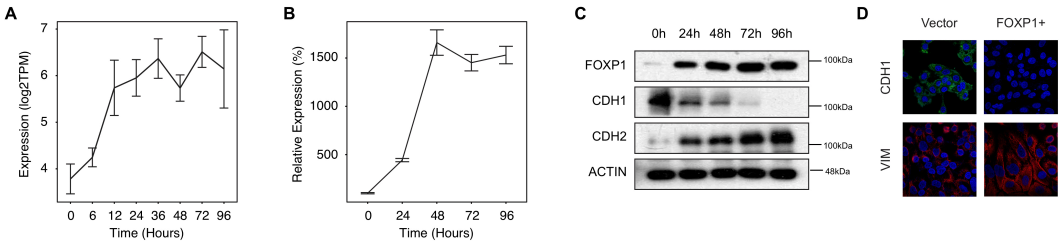


Supplementary Figure 1. **FOXP1 is a critical inducer of EMT in A549 cells.**
(A) RNA-seq data showing monotonic upregulation of FOXP1 during TGF-β-induced EMT in A549 cells. (B) Same as (A) using qRT-PCR. (C) Same as (A) for immunoblotting analysis. (D) Confocal microscopy images showing the upregulation of VIM protein and the downregulation of CDH1 protein in A549 cells overexpressing FOXP1. n = 3; error bars indicate the means ± s.d.

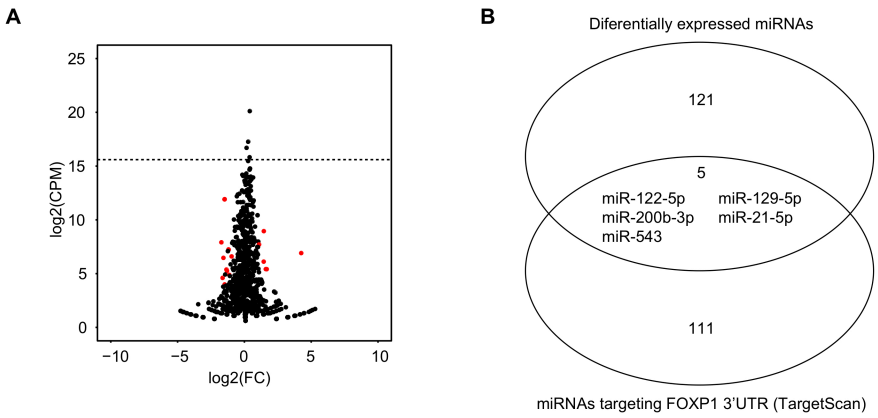


Supplementary Figure 2. **Sequencing analysis indicates that miR-21 is the key miRNA regulating EMT in A549 cells.**

(A) Volcano plot showing the differential expression of miRNAs at 24 h into TGF-β-induced EMT in A549 cells. The red dots represent miRNAs with a differential expression FDR < 0.05 and absolute log2-fold change > 1. The horizontal dotted line represents the log2(CPM) corresponding to 100 copies/cell. (B) Venn diagram showing the overlap between the miRNAs that were differentially expressed at 96 h into TGF-β-induced EMT in A549 cells and the miRNAs predicted by targetScan to regulate FOXP1.

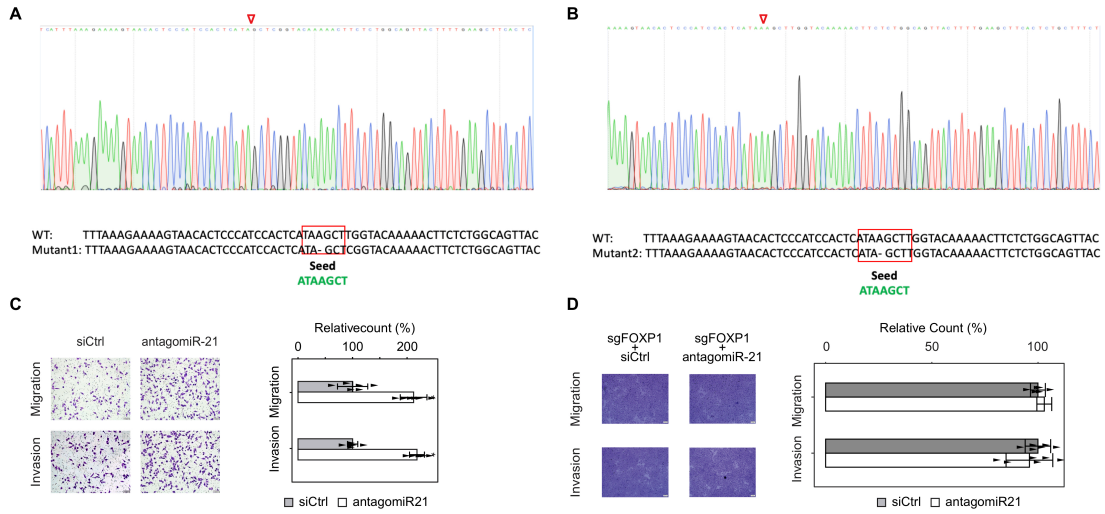


Supplementary Figure 3. **Sequencing traces of the CRISPR/Cas9 edited miR-21 binding site in FOXP1 3'UTR.**

(A) and (B) showing traces of genomic sequence surrounding the miR-21 binding site in FOXP1 3'UTR (upper panels) and corresponding primary sequences (lower panels) for the two alleles of a representative clone. Red boxes highlight the mutated miR-21 binding sites. Red triangles mark the mutation sites in sequencing traces. (C) A549 cells undergoing TGF-β-induced EMT were treated with an antagomiR targeting miR-21 and subjected to a migration assay (upper panel) and invasion assay (lower panel). Scale bars: 100 μm. The migrated or invaded cells were quantified (bar charts). n = 6. (D) A549 cells whose miR-21 binding site in FOXP1 has been mutated by CRISPR/Cas9 undergoing TGF-β-induced EMT were treated with an antagomiR targeting miR-21 and subjected to a migration assay (upper panel) and invasion assay (lower panel). Scale bars: 20 μm. The migrated or invaded cells were quantified (bar charts). n = 6. error bars indicate the means ± s.d. * $p < 0.01$, determined using a two-tailed Student's *t*-test.

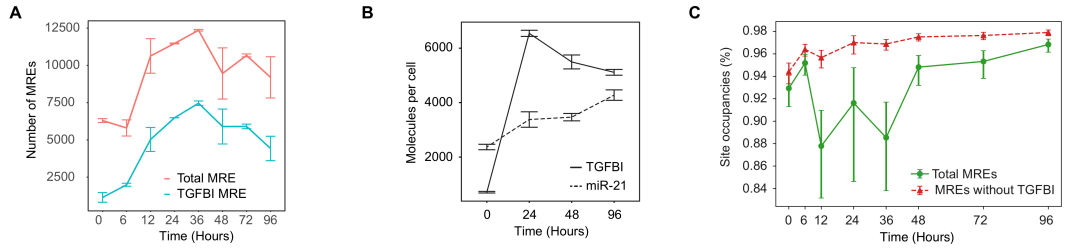


Supplementary Figure 4. **Dynamically induced mRNAs as ceRNA regulators of EMT in A549 cells.**

(A) Graph showing the number of miR-21 MREs extrapolated from RNA-seq data during TGF-β-induced EMT in A549 cells using pictar-based predictions. (B) Absolute quantification of the numbers of TGFBI mRNA and miR-21 transcripts during TGF-β-induced EMT in A549 cells. (C) Graph showing the dynamics of modeled 8-mer miR-21 binding site occupancy during TGF-β-induced EMT in A549 cells using pictar-based predictions. n = 3; error bars indicate the means ± s.d.

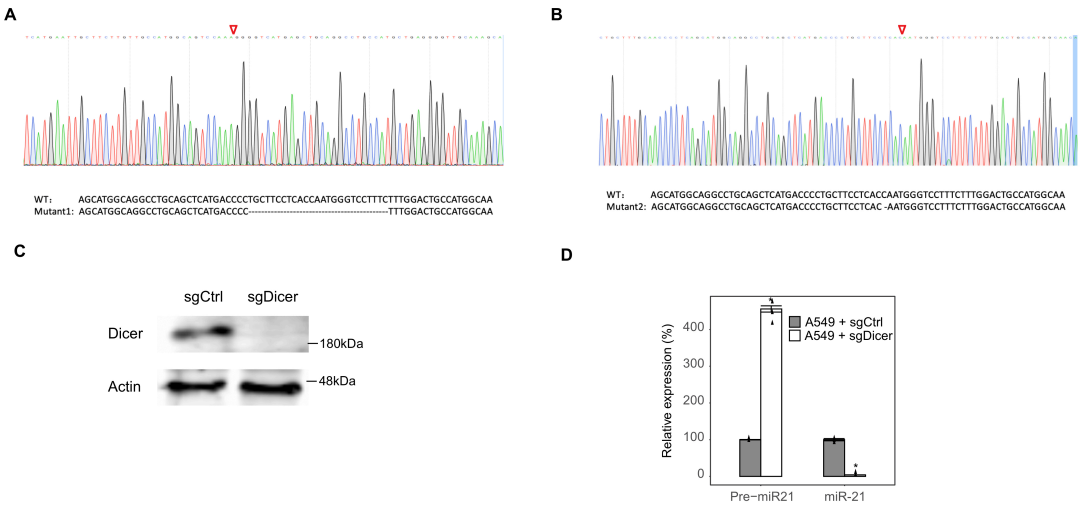


Supplementary Figure 5. **Knockdown of DICER1 abolishes ceRNA effects in A549 cells.**

(A) and (B) showing traces of genomic sequences of edited DICER1 coding region (upper panels) and corresponding primary sequences (lower panels) for the two alleles of a representative clone. Red triangles mark the mutation sites in sequencing traces. (C) Western blot showing the lack of DICER1 protein in edited A549 cells. (D) Barcharts showing the effects of DICER1 knockout on pre- and mature miRNA expression. n = 3; error bars indicate the means ± s.d. * $p < 0.01$, determined using a two-tailed Student's *t*-test.

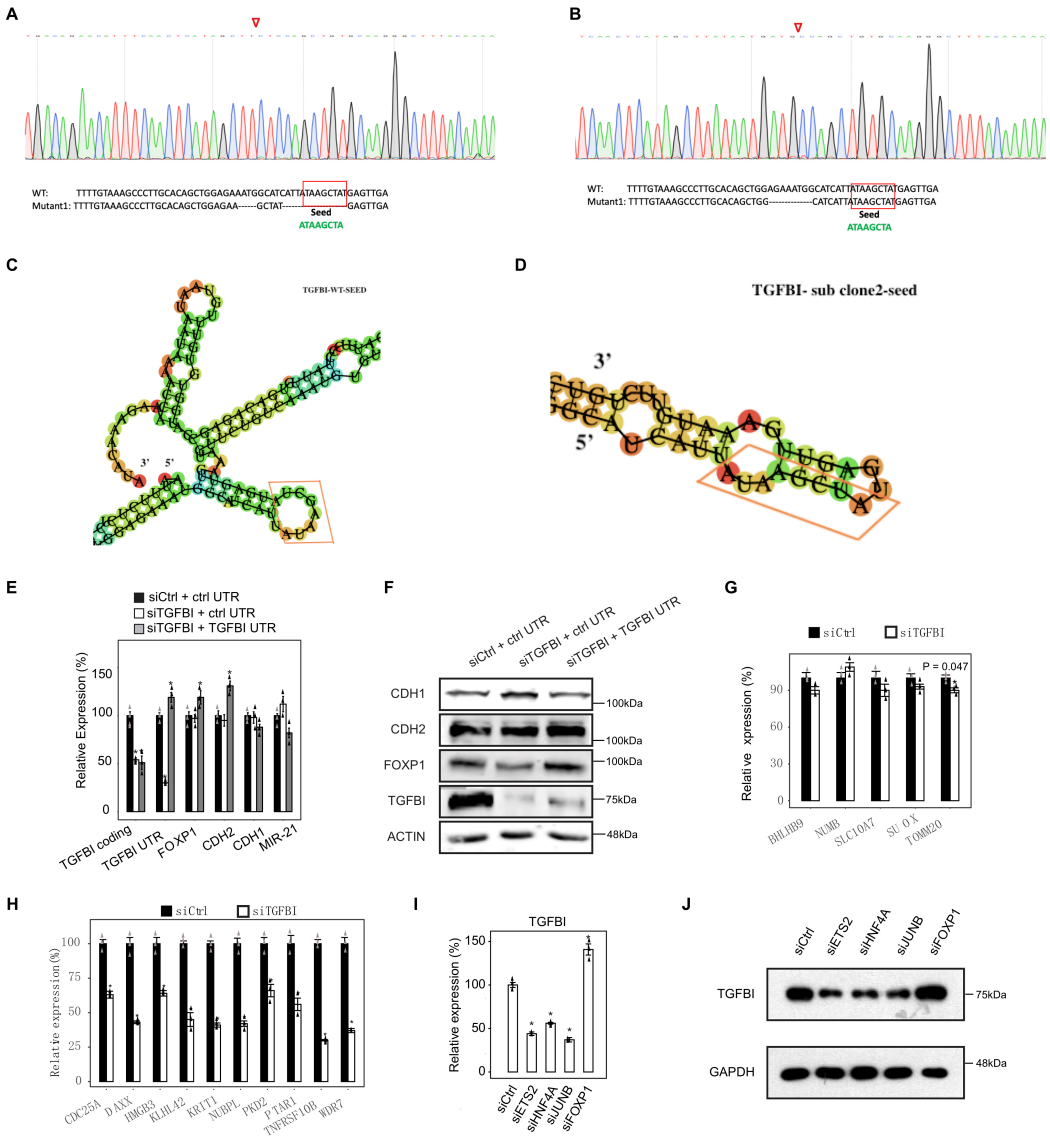


Supplementary Figure 6. **Mutating miR-21 binding site in TGFBI 3'UTR abolishes ceRNA effects in A549 cells.**

(A) and (B) showing traces of genomic sequence near the mutated miR-21 binding site in TGFBI 3'UTR (upper panels) and corresponding primary sequences (lower panels) for the two alleles of a representative clone. Red boxes highlight the mutated miR-21 binding sites. Red triangles mark the mutation sites in sequencing traces. (C) RNAduplex predicted secondary structure showing that the seed of miR-21 binding site in TGFBI 3'UTR is located in a loop region in wildtype cells. (D) RNAduplex predicted secondary structure showing that the mutated TGFBI 3'UTR as showed in (B) relocates the seed of miR-21 binding site to a stem region. (E) Graph showing the level of indicated RNAs in A549 cells during TGF-β-induced EMT subjected to indicated treatments using cells whose miR-21 binding site has been mutated with CRISPR/Cas9.

(F) Same as (E) for the immunoblotting analysis. (G) Graph showing the level of mRNAs for genes not targeted by miR-21 in A549 cells after knockdown of TGFBI. (H) same as (G) for known miR-21 target genes. (I) Graph showing the levels of TGFBI mRNA in A549 cells during TGF-β-induced EMT after silencing ETS2, HNF4A, JUNB or FOXP1 expression using specific siRNAs. (J) same as (I ) for immunoblotting analysis. n = 3; error bars indicate the means ± s.d. * $p < 0.01$, determined using a two-tailed Student's *t*-test.

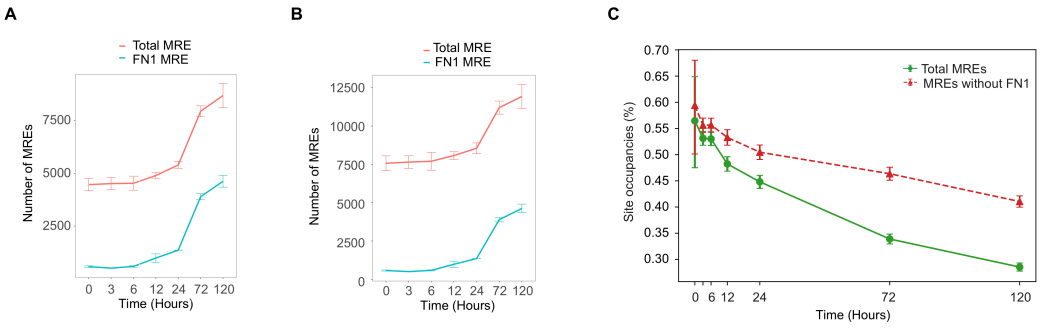


Supplementary Figure 7. **Dynamically induced mRNAs as ceRNA regulators of EMT in MCF10A cells.**

(A) Graph showing the number of miR-200c MREs extrapolated from microarray data during TGF-β-induced EMT in MCF10A cells using pictar-based predictions. (B) Graph showing the number of miR-200c MREs extrapolated from microarray data during TGF-β-induced EMT in MCF10A cells using targetScan-based predictions. (C) Graph showing the dynamics of modeled 8-mer miRNA binding site occupancy during TGF-β-induced EMT in MCF10A cells using targetScan-based predictions. n = 3; error bars indicate the means ± s.d.

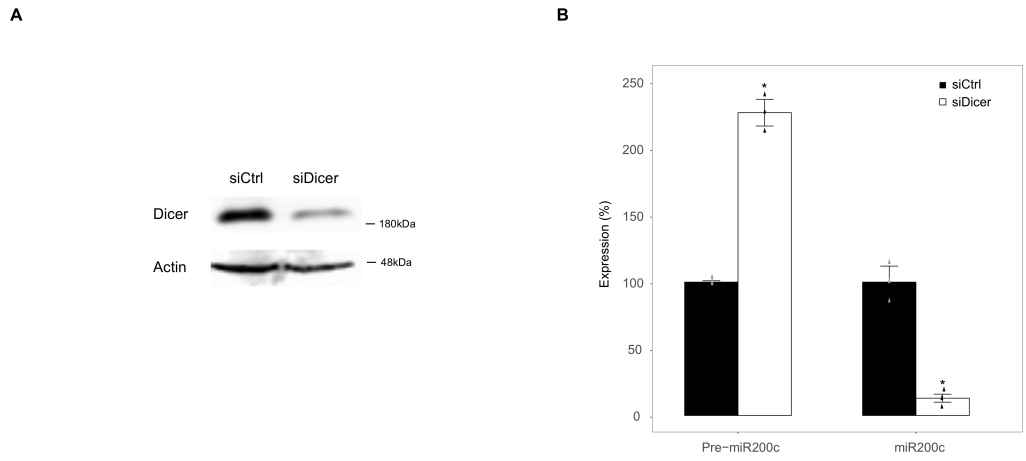


Supplementary Figure 8. **Knockdown of DICER1 abolish ceRNA effects in MCF10A cells.**

(A) Western blot showing the lack of DICER1 protein in treated MCF10A cells. (B) Barcharts showing the effects of DICER1 knockdown on pre- and mature miRNA expression. n = 3; error bars indicate the means ± s.d. * $p < 0.01$, determined using a two-tailed Student's *t*-test.

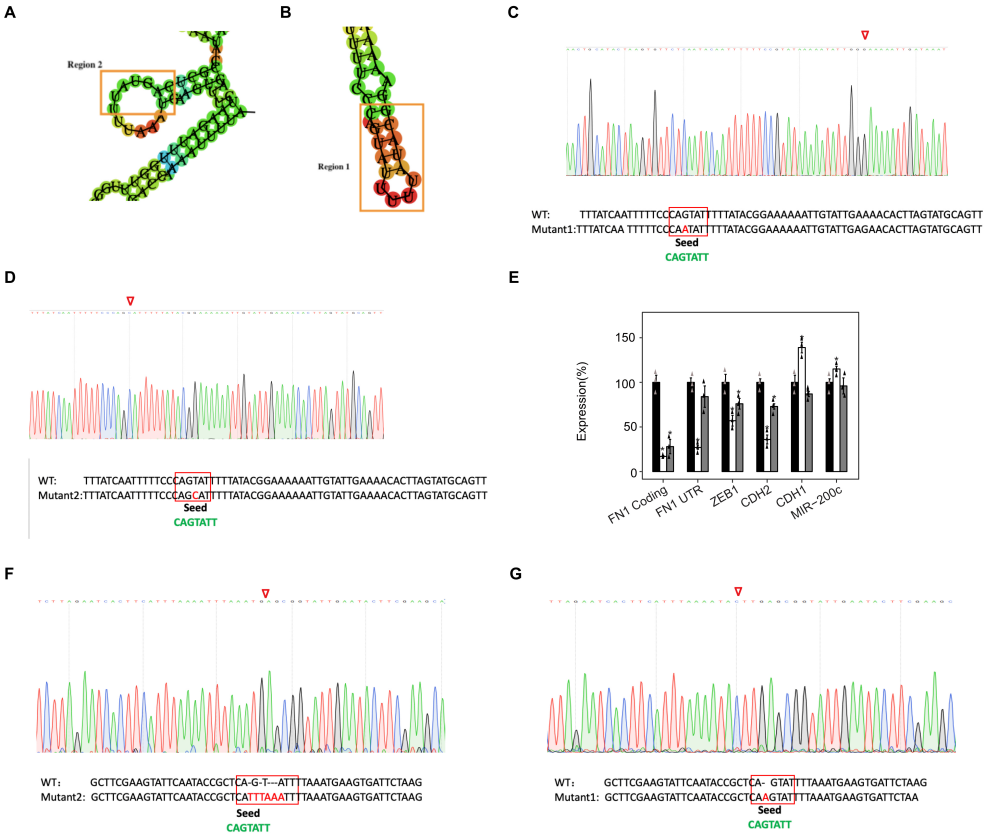


Supplementary Figure 9. **Mutating miR-200c binding site in FN1 3'UTR in MCF10A cells.**

(A) RNAduplex predicted secondary structure showing that the seed of the highly conserved miR-200c binding site in FN1 3'UTR is located in a loop region in wildtype cells. (B) RNAduplex predicted secondary structure showing that the seed of the poorly conserved miR-200c binding site in FN1 3'UTR is located in a stem region in wildtype cells. (C) and (D) showing traces of genomic sequence near the poorly conserved miR-200c binding site in FN1 3'UTR (upper panels) and corresponding primary sequences (lower panels) for the two alleles of a representative clone. Red boxes highlight the mutated miR-200c binding sites. Red triangles mark the mutation sites in sequencing traces. (E) Graph showing the level of indicated RNAs in MCF10A cells during TGF-β-induced EMT subjected to indicated treatments using cells whose poorly conserved miR-200c binding site has been mutated with CRISPR/Cas9. (F) and (G) same as (C) and (D) for the highly conserved miR-200c binding site in FN1 3'UTR. n = 3; error bars indicate the means ± s.d. * $p < 0.01$, determined using a two-tailed Student's *t*-test.

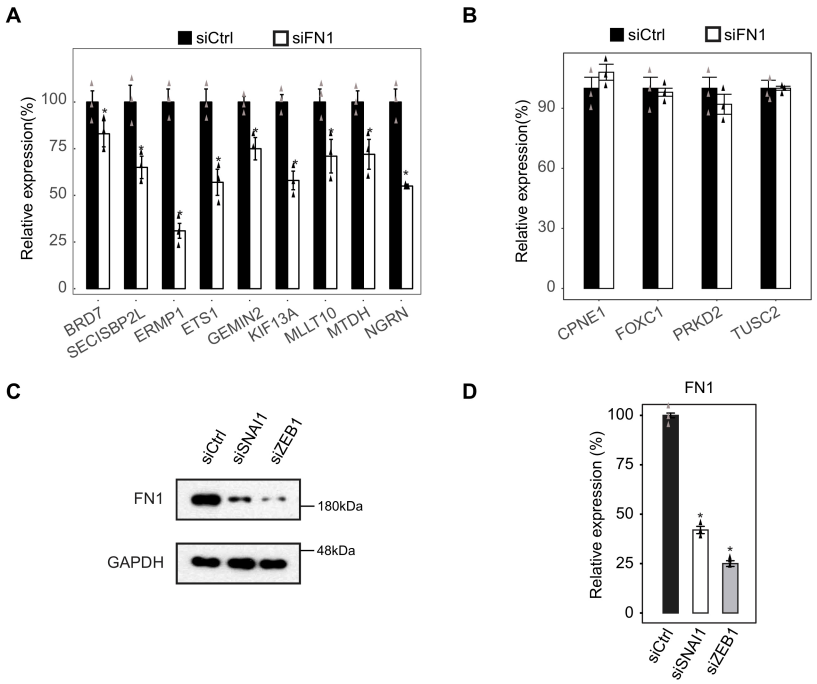


Supplementary Figure 10. **Mutating miR-200c binding site in FN1 3'UTR abolishes ceRNA effects in A549 cells.**

(A) Graph showing the level of RNAs for genes targeted by miR-200c in MCF10A cells after knockdown of FN1. (B) same as (A) for genes not targeted by miR-200c. (C) Immunoblotting analysis showing the abundance of FN1 protein in MCF10A cells during TGF-β-induced EMT after silencing SNAI1 or ZEB1 expression using specific siRNAs. (D) Same as (C) for FN1 mRNA. n = 3; error bars indicate the means ± s.d. * $p < 0.01$, determined using a two-tailed Student's *t*-test.

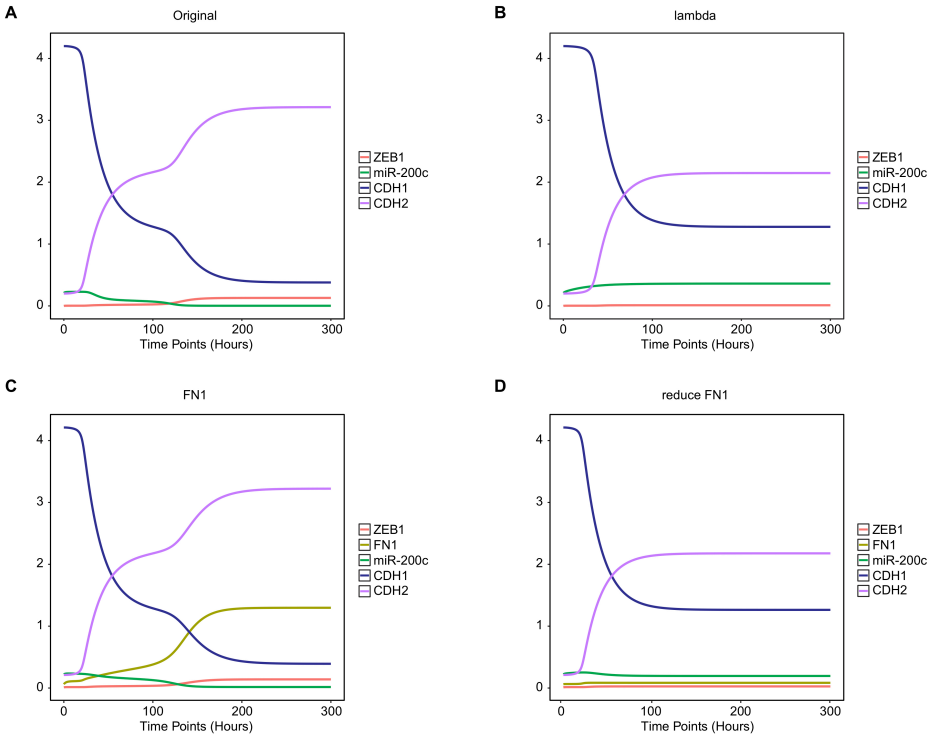


Supplementary Figure 11. **Simulated time-course dynamics of EMT genes.**
(A) Graph showing the time-course expression of key EMT genes during a 300h simulation using the model originally developed by Zhang et al. (B) Same as (A) but with lambda(1-5) increased from 0.5 to 0.9 to increase the half-life of miR-200c. (C) Graph showing the time-course expression of key EMT genes during a 300h simulation using the model incorporating FN1. (D) Same as (C) but with the FN1 degradation rate constant increased to 1 to simulate FN1 knockdown.

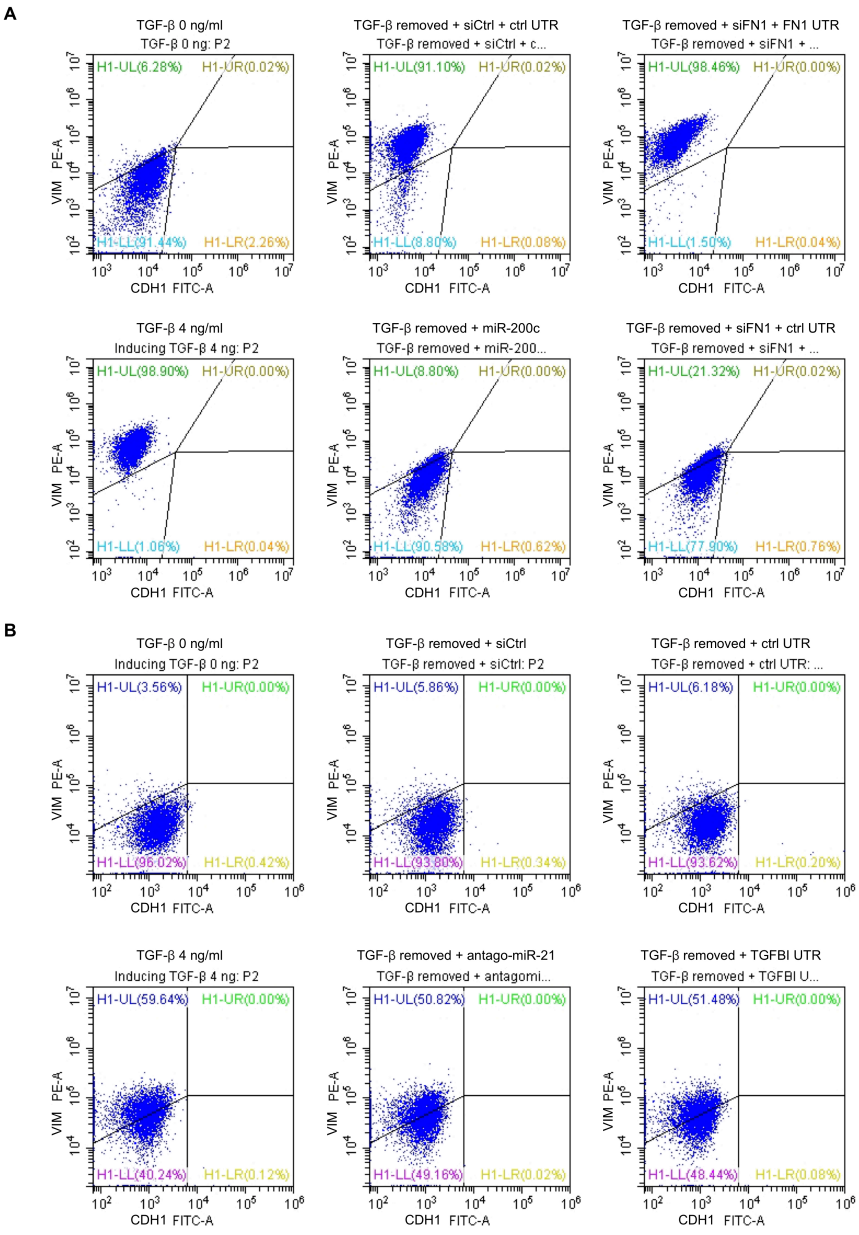


Supplementary Figure 12. **The stoichiometry between ceRNA and miRNA determines EMT reversibility.**

(A) MCF10A cells were treated with 0 or 4 ng/ml TGF-β for 7 days to induce EMT, followed by the indicated treatment for 3 days. The abundance of E-cadherin and Vimentin was analyzed via flow cytometry. The pictures are representative of three biological replicates. (B) Same as (A) for A549 cells.

**Supplementary Tables.**

**Supplementary Table 1.** Representative TPM of miR-21 target mRNAs during EMT in A549 cells.*

| Symbol | Isoform | 0h | 6h | 12h | 24h | 36h | 48h | 72h | 96h |
|---|---|---|---|---|---|---|---|---|---|
| TGFBI | ENST00000442011 | 288.48 | 748.27 | 1621.84 | 2721.68 | 3237.3 | 3215.27 | 2618.61 | 1409.31 |
| VCL | ENST00000372755 | 71.95 | 76.95 | 135.5 | 147.15 | 100.32 | 88.37 | 96.67 | 73.64 |
| TGFBI | ENST00000506699 | 8.03 | 49.29 | 64.87 | 99.12 | 105.41 | 80.36 | 59.71 | 22.94 |
| RTN4 | ENST00000317610 | 59.61 | 50.22 | 64.18 | 63.05 | 58.62 | 50.88 | 56.7 | 55.95 |
| JAG1 | ENST00000254958 | 12.43 | 17.87 | 28.31 | 43.23 | 46.99 | 41.68 | 55.62 | 38.55 |
| MPRIP | ENST00000341712 | 31.49 | 32.11 | 34.79 | 41.31 | 29.51 | 15.41 | 18.23 | 13.1 |
| RAB11A | ENST00000564910 | 36.62 | 34.39 | 35.67 | 38.19 | 33.09 | 34.41 | 36.72 | 29.34 |
| TGFB2 | ENST00000366930 | 22.27 | 24.04 | 28.17 | 34.7 | 31.43 | 29.33 | 25.49 | 16.73 |
| SCRN1 | ENST00000242059 | 36.55 | 29.34 | 30.19 | 28.16 | 27.42 | 25.93 | 24.73 | 21.02 |
| TGFBI | ENST00000504411 | 3.66 | 11.43 | 19.47 | 25.77 | 27.28 | 22.59 | 10.99 | 4.14 |
| BMPR2 | ENST00000374580 | 7.17 | 14.26 | 18.88 | 23.74 | 21.26 | 11.38 | 14.13 | 6.09 |
| STAG2 | ENST00000371157 | 19.46 | 14.51 | 20.31 | 20.33 | 19.99 | 19.29 | 15.66 | 13.12 |
| UBE2D3 | ENST00000394803 | 19.31 | 23.89 | 23.6 | 19.26 | 13.71 | 17.86 | 14.45 | 14.92 |
| RAB11A | ENST00000261890 | 20.22 | 16.8 | 19.07 | 18.71 | 19.59 | 19.74 | 19.46 | 14.5 |
| MPRIP | ENST00000395811 | 17.13 | 8.26 | 12.12 | 18.68 | 16.06 | 9.11 | 10.27 | 5.71 |
| RAB11A | ENST00000569896 | 13.92 | 15.79 | 15.3 | 18.45 | 17.53 | 18.2 | 15.2 | 15.14 |
| KPNA4 | ENST00000334256 | 17.23 | 17.72 | 18.81 | 16.82 | 13.48 | 12.01 | 12.6 | 9.82 |
| SOCS6 | ENST00000397942 | 16.15 | 11.12 | 13.42 | 15.99 | 23.04 | 30.64 | 26.43 | 21.1 |
| MSH2 | ENST00000233146 | 26.22 | 22.92 | 18.05 | 15.81 | 15.41 | 16.61 | 17.61 | 14.48 |
| LANCL1 | ENST00000450366 | 18.22 | 13.3 | 12.39 | 13.4 | 13.74 | 15.23 | 13.83 | 14.85 |
| SMAD7 | ENST00000262158 | 5.14 | 11.44 | 11.67 | 12.77 | 10.47 | 7.17 | 9.98 | 5.78 |
| YAP1 | ENST00000282441 | 10.67 | 7.26 | 9.98 | 10.95 | 8.96 | 10.1 | 10.71 | 9.36 |
| UBE2D3 | ENST00000394801 | 11.37 | 12.47 | 10.82 | 10.63 | 11.56 | 8.82 | 12.47 | 11.92 |
| HIPK3 | ENST00000303296 | 10.03 | 9.62 | 6.75 | 10.44 | 6.37 | 10.9 | 9.97 | 4.96 |

* Only isoforms with TPM > 10 at 24h into EMT are shown. Data is taken from replicate 1 of GSE69667.

**Supplementary Table 2.** MREs for miR-21 derived from TargetScan during EMT in A549 cells.*

| Time | # MREs from TGFBI | Total # of MREs | # of increased MREs from TGFBI comparing to 0h | Total # of increased MREs comparing to 0h | Percentage of increased MREs contributed by TGFBI |
|---|---|---|---|---|---|
| 0h | 498 | 1,554 | 0 | 0 | NA |
| 6h | 872 | 1,716 | 373 | 161 | 230% |
| 12h | 2,201 | 3,577 | 1,702 | 2,022 | 84% |
| 24h | 2,842 | 4,070 | 2,343 | 2,516 | 93% |
| 36h | 3,271 | 4,469 | 2,772 | 2,915 | 95% |
| 48h | 2,587 | 3,447 | 2,088 | 1,892 | 110% |
| 72h | 2,587 | 3,723 | 2,088 | 2,168 | 96% |
| 96h | 1,936 | 3,057 | 1,438 | 1,502 | 95% |

* MREs were before scaling with absolute qPCR data.

**Supplementary Table 3.** Representative TPM of miR-200c target mRNAs during EMT in MCF10A cells.*

| Symbol | Isoform | 0h | 3h | 6h | 12h | 24h | 72h | 120h |
|---|---|---|---|---|---|---|---|---|
| FN1 | ENST00000336916 | 218.15 | 194.4696674 | 222.1218974 | 388.1095348 | 517.3348997 | 1490.119701 | 1744.526457 |
| FN1 | ENST00000357867 | 217.48 | 193.8723964 | 221.4396986 | 386.9175413 | 515.7460187 | 1485.543124 | 1739.168526 |
| FN1 | ENST00000456923 | 206.22 | 183.8346771 | 209.9746857 | 366.8849336 | 489.0433327 | 1408.629313 | 1649.123291 |
| NPM1 | ENST00000517671 | 1236.67 | 1306.725747 | 1246.622555 | 1280.029453 | 1234.432937 | 1257.135243 | 1411.762355 |
| FN1 | ENST00000421182 | 111.48 | 99.37876932 | 113.509737 | 198.3334904 | 264.3708211 | 761.4877115 | 891.4958031 |
| FN1 | ENST00000443816 | 100.64 | 89.71545877 | 102.4723711 | 179.0481026 | 238.6641499 | 687.4427995 | 804.8092718 |
| FN1 | ENST00000323926 | 37.84 | 33.73244197 | 38.52895988 | 67.32094796 | 89.73620264 | 258.4741209 | 302.6031682 |
| NPM1 | ENST00000351986 | 193.56 | 204.5249223 | 195.117745 | 200.3464958 | 193.2098614 | 196.7631604 | 220.9649473 |
| RHOA | ENST00000418115 | 166.59 | 170.4329788 | 161.6843865 | 180.5195562 | 163.8056198 | 177.9292789 | 195.4089932 |
| YWHAQ | ENST00000238081 | 143.39 | 162.9973397 | 166.7990172 | 168.012319 | 162.0424524 | 168.1526637 | 190.0838966 |
| SERF2 | ENST00000409614 | 150.19 | 141.515457 | 153.0885569 | 131.8141477 | 131.6727301 | 151.8285129 | 153.6924672 |
| HSPA9 | ENST00000297185 | 150.33 | 152.4771205 | 152.988219 | 148.5528113 | 157.6793856 | 145.5471835 | 169.809349 |
| DDIT4 | ENST00000307365 | 172.28 | 141.2570047 | 132.1644885 | 136.3792126 | 153.148988 | 138.1825242 | 79.99864564 |
| FSTL1 | ENST00000295633 | 45.06 | 51.53215074 | 66.64270324 | 78.45239938 | 90.06475148 | 123.5215759 | 139.4024721 |
| NPM1 | ENST00000296930 | 116.74 | 123.3531692 | 117.6795079 | 120.8330746 | 116.5288243 | 118.6718917 | 133.2684849 |
| GDI2 | ENST00000380191 | 118.51 | 113.4256029 | 122.4551297 | 115.3985197 | 109.5783983 | 107.3015832 | 120.5353254 |
| HNRNPK | ENST00000376281 | 97.29 | 123.0332702 | 97.88238055 | 88.60202383 | 95.71614136 | 97.94893847 | 102.0991836 |
| ETF1 | ENST00000360541 | 87.68 | 88.39490636 | 82.10596601 | 80.48847112 | 84.8576093 | 86.61150113 | 95.89569855 |
| HNRNPK | ENST00000360384 | 81.4 | 102.9387213 | 81.89562932 | 74.13099743 | 80.08319361 | 81.95131659 | 85.4237182 |
| FSTL1 | ENST00000424703 | 29.22 | 33.41698723 | 43.21570769 | 50.87392609 | 58.40417306 | 80.09987676 | 90.39814101 |
| MSN | ENST00000360270 | 61.04 | 71.61872518 | 76.88584587 | 73.3466566 | 66.7003055 | 79.1416521 | 75.81215871 |
| YWHAB | ENST00000353703 | 67.12 | 67.96575468 | 79.73754397 | 69.97046353 | 71.86891001 | 75.81649932 | 104.2279166 |
| SCD | ENST00000370355 | 69.6 | 75.54895952 | 73.47699757 | 69.63295152 | 75.07596693 | 75.49159188 | 60.76853911 |
| HNRNPH1 | ENST00000442819 | 67.5 | 69.62688099 | 65.77859133 | 66.20859737 | 80.10018398 | 73.95756061 | 84.43658565 |
| SERINC1 | ENST00000339697 | 57.82 | 53.86475714 | 62.12141695 | 58.48621947 | 64.0946661 | 73.87149167 | 80.16246806 |
| HAS2 | ENST00000303924 | 11.01 | 8.799935081 | 10.08342441 | 14.62964421 | 22.39759645 | 69.58670458 | 67.43490269 |
| PRKAR1A | ENST00000358598 | 57.08 | 62.47690424 | 68.11480071 | 64.32878981 | 78.43650994 | 69.4510315 | 93.59488329 |
| DHX9 | ENST00000367549 | 62.67 | 60.31315929 | 58.02458044 | 60.25724736 | 60.06180501 | 61.36469369 | 62.48261492 |
| AHNAK | ENST00000378024 | 64.33 | 50.31201288 | 41.96601294 | 45.5871644 | 64.7337667 | 60.46195277 | 48.89967866 |
| FERMT2 | ENST00000341590 | 34.81 | 39.05346554 | 39.39222348 | 44.93233922 | 55.91425309 | 60.00271 | 65.19608486 |
| HNRNPU | ENST00000440865 | 83.58 | 72.7714877 | 58.41560554 | 61.96430465 | 82.70610042 | 59.3497176 | 37.55328565 |
| MFAP5 | ENST00000359478 | 1.92 | 1.749122893 | 10.745876 | 1.362589197 | 1.440498374 | 54.1417911 | 0.535907629 |
| RAC1 | ENST00000348035 | 56.39 | 50.52308793 | 52.15738695 | 54.91387835 | 46.61281219 | 53.35004323 | 57.34147416 |
| SSR3 | ENST00000265044 | 42.44 | 47.31662733 | 43.07088867 | 42.58786893 | 36.57239432 | 51.50046239 | 54.43564608 |
| APLP2 | ENST00000278756 | 50 | 42.67900914 | 47.88043756 | 51.68234377 | 55.36853395 | 50.88366248 | 45.5221682 |
| PLS3 | ENST00000355899 | 52.13 | 55.24744754 | 57.00376948 | 55.55695374 | 59.33643325 | 50.67590928 | 56.8522669 |
| SRSF1 | ENST00000582730 | 59.45 | 54.49509273 | 47.97438992 | 55.56535187 | 58.22428338 | 50.03156926 | 56.2999231 |
| YWHAG | ENST00000307630 | 52.13 | 46.80480648 | 44.63275078 | 50.45720699 | 58.91846177 | 49.40816013 | 39.23687753 |
| SERF2 | ENST00000339624 | 48.2 | 45.41610646 | 49.13022468 | 42.30269603 | 42.25731135 | 48.72584275 | 49.32403569 |
| LAMC1 | ENST00000258341 | 50.89 | 49.74757564 | 47.05823871 | 43.66267328 | 53.13061409 | 47.78911857 | 44.53720429 |
| LAMC1 | ENST00000258341 | 50.89 | 49.74757564 | 47.05823871 | 43.66267328 | 53.13061409 | 47.78911857 | 44.53720429 |
| RAP1B | ENST00000393436 | 43.68 | 43.70123824 | 45.51455976 | 42.12859086 | 40.77725705 | 46.97169 | 55.35045206 |
| SHC1 | ENST00000368453 | 38.75 | 42.98141461 | 42.22759247 | 36.42219795 | 43.59413103 | 46.50348379 | 42.40591604 |
| YME1L1 | ENST00000376016 | 38.5 | 39.44502162 | 38.27567762 | 37.02989186 | 39.82341519 | 45.84909843 | 39.15577724 |
| ANLN | ENST00000265748 | 36.34 | 36.57354212 | 39.05144624 | 40.69339151 | 45.03275046 | 43.67700781 | 59.92151983 |
| PTPN11 | ENST00000351677 | 36.14 | 39.7057089 | 40.90019355 | 34.52618887 | 37.13749112 | 41.62203628 | 42.17728724 |
| SHC1 | ENST00000448116 | 32.2 | 35.71616905 | 35.08976716 | 30.26567159 | 36.22531662 | 38.64289492 | 35.2379483 |
| FRMD6 | ENST00000395718 | 25.58 | 29.64869257 | 29.87433362 | 27.99160091 | 29.02920235 | 37.93865501 | 48.03260161 |
| PCNP | ENST00000265260 | 33.99 | 34.13669932 | 35.11046938 | 30.34306699 | 31.98796271 | 37.69473224 | 37.1741179 |

* Top 50 isoforms at 72h into EMT are shown.

**Supplementary Table 4.** MREs for miR-200c derived from TargetScan during EMT in MCF10A cells.*

| Time | # MREs from FN1 | Total # of MREs | # of increased MREs from FN1 comparing to 0h | Total # of increased MREs comparing to 0h | Percentage of increased MREs contributed by FN1 |
|---|---|---|---|---|---|
| 0h | 893 | 11678 | 0 | 0 | NA |
| 3h | 796 | 11828 | -97 | 149 | -64% |
| 6h | 909 | 11869 | 16 | 190 | 8% |
| 12h | 1589 | 12572 | 696 | 894 | 77% |
| 24h | 2119 | 13243 | 1225 | 1564 | 78% |
| 72h | 6104 | 17379 | 5210 | 5700 | 91% |
| 120h | 7146 | 18388 | 6252 | 6709 | 93% |

* MREs were before scaling with absolute qPCR data.

**Supplementary Table 5.** MiRNA expression in MCF10A cells (GSE50064).

| | normalized count |
|---|---|
| miR-378a-3p | 5,886,078 |
| miR-378c | 5,875,199 |
| miR-378d | 5,868,998 |
| let-7a-5p | 3,087,464 |
| let-7c | 2,929,684 |
| let-7f-5p | 1,457,612 |
| miR-103a-3p | 559,644 |
| miR-103b | 559,644 |
| miR-107 | 541,327 |
| miR-21-5p | 486,038 |
| miR-27a-3p | 478,586 |
| miR-27b-3p | 477,975 |
| miR-100-5p | 221,489 |
| miR-200c-3p | 211,178 |

**Supplementary Table 6.** Conserved miRNA binding sites in ZEB1 3'UTR as predicted by targetScan 7.2.

| miRNA family | Total | 8mer | 7mer-m8 | 7mer-A1 |
|---|---|---|---|---|
| miR-200bc-3p/429 | 5 | **3** | **2** | 0 |
| miR-141-3p/200a-3p | 3 | **1** | **2** | 0 |
| miR-183-5p.2 | 2 | 0 | **1** | **1** |
| miR-139-5p | 2 | **1** | **1** | 0 |
| miR-101-3p.1 | 2 | **1** | 0 | **1** |
| miR-101-3p.2 | 2 | 0 | **2** | 0 |
| miR-144-3p | 2 | **1** | 0 | **1** |
| miR-124-3p.2/506-3p | 1 | 0 | 0 | **1** |
| miR-96-5p/1271-5p | 1 | 0 | **1** | 0 |
| miR-205-5p | 1 | **1** | 0 | 0 |
| miR-183-5p.1 | 1 | 0 | **1** | 0 |
| miR-128-3p | 1 | 0 | **1** | 0 |
| miR-150-5p | 1 | **1** | 0 | 0 |
| miR-223-3p | 1 | 0 | 0 | **1** |
| miR-130-3p/301-3p/454-3p | 1 | 0 | 0 | **1** |
| miR-199-3p | 1 | 0 | **1** | 0 |
| miR-142-3p.1 | 1 | 0 | 0 | **1** |
| miR-455-3p.1 | 1 | 0 | **1** | 0 |
| miR-199-5p | 1 | 0 | **1** | 0 |
| miR-143-3p | 1 | 0 | 0 | **1** |
| miR-181-5p | 1 | 0 | 0 | **1** |
| miR-23-3p | 1 | 0 | **1** | 0 |
| miR-194-5p | 1 | 0 | 0 | **1** |
| miR-216a-5p | 1 | 0 | **1** | 0 |
| miR-203a-3p.2 | 1 | 0 | **1** | 0 |
| miR-203a-3p.1 | 1 | **1** | 0 | 0 |
| miR-204-5p/211-5p | 1 | **1** | 0 | 0 |
| miR-802 | 1 | 0 | 0 | **1** |

**Supplementary Table 7.** Parameters and variables adjusted or added in the EMT model incorporating FN1.

| Parameter or variable | Description | Original Value | Adjusted/added value |
|---|---|---|---|
| Lamda1-5 | Recycling ratio of miR-200 from degraded miR-200-ZEB1 complex | 0.5 | 0.9 |
| Lamdafn1 | Recycling ratio of miR-200 from degraded miR-200-FN1 complex | NA | 0.86 |
| $k0_{fn1}$ | Transcription rate constant of Fn1 | NA | 0.05 μM/hr |
| $kd_{fn1}$ | Degradation rate constant of free Fn1 | NA | 0.08/hr |
| $kd_{fR1}$ | Degradation rate constant of Fn1-miR-200 complex | NA | 0.9/hr |
| $K_{fn1}$ | Binding rate constant of miR-200 to Fn1 | NA | 10 /μM |
| $ks_{fn1}$ | Transcription rate constant of SNAI1 on Fn1 | NA | 0.02 μM/hr |
| $kz_{fn1}$ | Transcription rate constant of ZEB1 on Fn1 | NA | 0.04 μM/hr |
| $Js_{fn1}$ | Michaelis constant of SNAI1 regulation of Fn1 | NA | 0.2 μM |
| $Jz_{fn1}$ | Michaelis constant of ZEB1 regulation of Fn1 | NA | 0.5 μM |
| $[Fn1]_t$ | Initial concentration of Fn1 transcripts | NA | 0.05 μM |

*NA indicates that the parameter or variable is not in the EMT model of Zhang et al.

## Supplementary Note. ODEs describing the EMT model incorporating FN1.

```
# The model was based on the CBS EMT model developed at Dr. Jianhua Xing's group.
# Please refer to Zhang, J.Y. et al. TGF-beta-induced epithelial-to-mesenchymal
# transition proceeds through stepwise activation of multiple feedback loops. Sci
# Signal 7 (2014).

p TGF0=0
p Ks=100, lamdas=0.5

#Time scale for mRNA and miRNA binding and unbinding, which is assumed very fast.

p Timescale=1000
TGFt=TGF+TGF0
miR34=miR34t-SR1
snail=snailt-SR1
snailt'= k0_snail + k_snail*(TGFt/J_snail0)^2 /(1+(TGFt/J_snail0)^2 )/(1+SNAIL/J_snail1)-
kd_snail*snail-kd_SR1*SR1

SNAIL'= k_SNAIL*snail-kd_SNAIL*SNAIL

miR34t'= k0_34 + k_34/( 1 + (SNAIL/J1_34)^2+ (ZEB/J2_34)^2)- kd_34*miR34-
kd_SR1*SR1+lamdas*kd_SR1*SR1

SR1'=Timescale*(Ks*snail*miR34-SR1)

 p k0_snail=.0006, k_snail=0.05, J_snail0=.62, J_snail1=.67, kd_snail=0.09, kd_SR1=0.9 ,

p k_SNAIL=17,  kd_SNAIL=1.66,

p k0_34=0.0012, k_34=0.012, J1_34=0.15, J2_34=0.36,  kd_34=0.035,


#########################################################################################
###

p K1=10, K2=10, K3=10, K4=10, K5=10

p lamda1=0.9, lamda2=0.9, lamda3=0.9, lamda4=0.9, lamda5=0.9

p dk_ZR1=0.9, dk_ZR2=0.9, dk_ZR3=0.9, dk_ZR4=0.9, dk_ZR5=0.9

 zebt'= k0_zeb + k_zeb*(SNAIL/J_zeb)^2 /( 1 + (SNAIL/J_zeb)^2 )- kd_zeb*zeb-dk_ZR1*5*ZR1-
dk_ZR2*10*ZR2-dk_ZR3*10*ZR3-dk_ZR4*5*ZR4-dk_ZR5*ZR5

ZEB'= k_ZEB*zeb-kd_ZEB*ZEB


ZR1'=Timescale*(K1*miR200*zeb-ZR1)

ZR2'=Timescale*(K2*miR200*ZR1-ZR2)

ZR3'=Timescale*(K3*miR200*ZR2-ZR3)

ZR4'=Timescale*(K4*miR200*ZR3-ZR4)

ZR5'=Timescale*(K5*miR200*ZR4-ZR5)
```

```
zeb=zebt-(5*ZR1+10*ZR2+10*ZR3+5*ZR4+ZR5)

 p k0_zeb=.003, k_zeb=0.06,  J_zeb=3.5,  kd_zeb=0.09,

p k_ZEB=17, J_ZEB=0.06,  kd_ZEB=1.66,

p k0_200=0.0002, k_200=0.02, J1_200=3.25, J2_200=0.2, kd_200=0.035,


###################################
# FN1 related parameters and ODEs#
###################################

p k0_fn1=0.05, kd_fn1=0.08, kd_fR1=0.9

p Kfn1=10

p ks_fn=0.02, kz_fn=0.04, Js_fn1=0.2, Jz_fn1=0.5

p lamdafn1=0.86

fnt'=k0_fn1+ks_fn*(SNAIL/Js_fn1)^2/(1+(SNAIL/Js_fn1)^2)+kz_fn*(ZEB/Jz_fn1)^2/(1+(ZEB/J
z_fn1)^2)-kd_fn1*fn1-kd_fR1*fR1

fn1=fnt-fR1

fR1'=Timescale*(Kfn1*miR200*fn1-fR1)

miR200t'= k0_200 + k_200/( 1 + (SNAIL/J1_200)^3 + (ZEB/J2_200)^2)-kd_200*miR200 -
dk_ZR1*5*ZR1-dk_ZR2*2*10*ZR2-dk_ZR3*3*10*ZR3-dk_ZR4*4*5*ZR4-
dk_ZR5*5*ZR5+lamda1*dk_ZR1*5*ZR1+lamda2*dk_ZR2*2*10*ZR2+lamda3*dk_ZR3*3*10*
ZR3+lamda4*dk_ZR4*4*5*ZR4+lamda5*dk_ZR5*5*ZR5-                kd_tgfR*tgfR+
lamdatgfR*kd_tgfR*tgfR-kd_fR1*fR1+lamdafn1*kd_fR1*fR1

miR200=miR200t-(5*ZR1+2*10*ZR2+3*10*ZR3+4*5*ZR4+5*ZR5)-tgfR-fR1

###################################################################################
####################

 p KTGF=20, TGF_flg=0

p k_tgf=0.05, kd_tgf=0.09, kd_tgfR=0.9,lamdatgfR=0.8

p k_TGF=1.6, kd_TGF=1,

tgft' = k_tgf - kd_tgf*tgf- kd_tgfR*tgfR

TGF' = k_TGF*tgf - kd_TGF*TGF

 tgf=tgft-tgfR

tgfR'=Timescale*(TGF_flg+KTGF*miR200*tgf-tgfR)
```

```
#############################################################################################
#####################

p k_ecad0=0.01, k_ecad1=0.15, k_ecad2=.05, J_ecad1=.2, J_ecad2=0.5,kd_ecad=.05,

p k_ncad0=0.01, k_ncad1=0.1, k_ncad2=.06, J_ncad1=.2, J_ncad2=0.5,kd_ncad=.05,

E_cadherin'=k_ecad0+k_ecad1/((SNAIL/J_ecad1)^2          +1)+k_ecad2/((ZEB/J_ecad2)^2+1)-
kd_ecad*E_cadherin

N_cadherin'=k_ncad0+k_ncad1*((SNAIL/J_ncad1)^2)/((SNAIL/J_ncad1)^2+1)+k_ncad2*((ZEB/
J_ncad2)^2)/((ZEB/J_ncad2)^2+1)-kd_ncad*N_cadherin

 init snailt=0,SNAIL=0,miR34t=0.37

init zebt=0,ZEB=0,miR200t=0.21,ZR1=0,ZR2=0,ZR3=0,ZR4=0,ZR5=0,ZR6=0

init tgfmt=0.07,TGF=0.03,tgfR=0.05,E_cadherin=4.2,N_cadherin=0.2

init fnt=0.05

done
```